

Non-Leptonic Decays of Bileptons

Gennaro Corcella^{(a)*}, Claudio Corianò^{(b)†},
Antonio Costantini^{(c)‡} and Paul H. Frampton^{(b)§}

^(a) INFN, Laboratori Nazionali di Frascati,
Via E. Fermi 54, 00044, Frascati (Rome), Italy.

^(b) Dipartimento di Matematica e Fisica ‘Ennio De Giorgi’,
Università del Salento, and INFN, Sezione di Lecce, Via Arnesano, 73100, Lecce, Italy.

^(c) Center for Cosmology, Particle Physics and Phenomenology (CP3),
Université Catholique de Louvain, Chemin du Cyclotron, B-1348, Louvain la Neuve,
Belgium

Abstract

We provide a detailed analysis of the decays of doubly-charged bilepton gauge bosons $Y^{\pm\pm}$, as predicted in models based on a $SU(3)_C \times SU(3)_L \times U(1)_X$ symmetry. In addition to the decay modes into same-sign lepton pairs, which were already investigated in scenarios wherein each branching ratio was about one third, there are, depending on the mass spectrum, possible non-leptonic decays which reduce the leptonic rates. These non-leptonic decays are typically into a light quark (antiquark) and a heavy TeV-scale antiquark (quark), which carries double lepton number and decays via virtual bileptons. We choose two benchmark points to represent the particle spectrum and present a phenomenological analysis of such decays. We find that, while the LHC statistics are too low, even in the high-luminosity phase, they can lead to a visible signal at a future 100 TeV hadron collider (FCC- hh). A more exhaustive exploration with a rigorous inclusion of tagging efficiencies, detector simulations and higher-order corrections to the partonic cross section, aiming at assessing the reach of LHC and FCC- hh for bileptons as a function of the model parameters, as well as a recast of four-top searches in terms of the bilepton model, are deferred to future work.

*gennaro.corcella@lnf.infn.it

†claudio.coriano@le.infn.it

‡antonio.costantini@uclouvain.be

§paul.h.frampton@gmail.com

1 Introduction

Bileptons appear in the model introduced in [1, 2] as spin-one gauge bosons which have the distinctive properties of $|Q| = |L| = 2$, where Q is electric charge and L the lepton number: their name became bileptons (from dileptons) in [3]. In the original paper [1] the model was named 331 model, being based on a $SU(3)_C \times SU(3)_L \times U(1)_X$ symmetry, while in [4] the authors have preferred calling it bilepton model, because it is necessary to select a well-defined embedding of the electric charge operator to characterise adequately the theory, and not only the gauge group.

The advantages of the bilepton model are the explanation for three quark-lepton families, as well as the asymmetry of the third quark family, and the necessity that the new physics must lie in the TeV range and cannot be pushed to a higher mass scale. The principal new particles which are predicted by this model and will be our concern hereafter are the gauge bileptons $Y^{\pm\pm}$ and the three extra quarks D , S and T with charges $Q = -4/3$, $-4/3$ and $+5/3$, respectively, and lepton number $L = +2$ (D and S) and -2 (T).

The present paper can be regarded as the third in a series after [4, 5] studying bilepton phenomenology. In fact, the most popular scenarios of physics Beyond the Standard Model, such as supersymmetry or Universal Extra Dimensions, have given no signal of new physics at the LHC, and therefore we find it mandatory investigating alternative scenarios, such as the bilepton model and the new particles contained in its spectrum. In detail, Ref. [4] explored the production at LHC of pairs of gauge bileptons, decaying into same-sign lepton pairs and accompanied by two jets. Ref. [5] added to the model Lagrangian an extra Higgs scalar sector, which is a sextet of $SU(3)_L$, leading to physical doubly-charged Higgs bosons. The phenomenology of scalar and gauge bileptons was studied in [5] in a scenario wherein both decay into same-sign lepton pairs with branching ratio $1/3$ for each lepton species. The final result was that the bilepton signal could be discriminated from the background, with the gauge bileptons dominating over the scalars¹

In this paper we shall concentrate on decays involving the extra quarks, in such a way to complete the exploration of final states yielded by bileptons and make a final statement on which signal one should look for at LHC and future colliders. We shall not account for scalar bileptons: in fact, while Higgs bosons with charge ± 2 are predicted in several models, doubly-charged gauge bosons are instead a rather unique feature of the model in [1]. Including doubly-charged Higgs bosons through a $SU(3)_L$ sextet as done in [5] is nevertheless straightforward.

¹See also Ref. [6] for an investigation on doubly-charged particles with different spin at LHC in the framework of simplified models.

In our analysis we need to estimate the masses of the bilepton M_Y and of the three quarks M_D , M_S and M_T . For M_Y there is a firm lower limit arising from two different low-energy experiments performed two decades ago. The first is muonium-antimuonium conversion $\mu^+e^- \rightarrow \mu^-e^+$ which can be mediated by bilepton exchange [7]; the second is the measurement of the Michel parameter ξ in muon decay $\mu^- \rightarrow e^-\bar{\nu}_e\nu_\mu$ which measures [8–10] the deviation from pure $(V - A)$ coupling, i.e. $(V - \xi A)$. The L -violating decay $\mu^- \rightarrow e^-\nu_e + \bar{\nu}_\mu$ can be mediated by virtual bilepton exchange and contribute to an effective $(V + A)$ part, hence leading to a departure of ξ below unity. By coincidence, both experiments agree on a lower mass limit $M_Y \geq 800$ GeV. As for high-energy colliders, at the LHC doubly-charged Higgs bosons were searched in a number of models by ATLAS [11] and CMS [12], under the assumption of a 100% leptonic rate. The ATLAS analysis [11], performed at 13 TeV and with an integrated luminosity $\mathcal{L} = 36 \text{ fb}^{-1}$, considered the so-called left-right symmetric model (LRSM) [13, 14] and its implementation in [15], with $H^{\pm\pm}$ coupling to either left- or right-handed leptons. Ref. [11] excluded $H_L^{\pm\pm}$ in the range 770-870 GeV and $H_R^{\pm\pm}$ in 660-760 GeV. As for CMS, limits between 800 and 820 GeV were determined at $\mathcal{L} = 12.9 \text{ fb}^{-1}$ [12]. More recently, in Ref. [16] the ATLAS Collaboration searched for doubly-charged Higgs bosons decaying into $W^\pm W^\pm$ pairs at $\mathcal{L} = 139 \text{ fb}^{-1}$, excluding them at 95% confidence level up to a mass of 350 GeV.

From a theoretical viewpoint, we know from [1] that the scale characterizing the symmetry breaking in the bilepton model is $\lesssim 4$ TeV, which may be regarded as analogous to the electroweak breaking scale $\langle H \rangle \sim 248$ GeV. Therefore, since the W mass is about $\sim \langle H \rangle / 3$, likewise $M_Y \sim 4 \text{ TeV} / 3 \sim 1.4 \text{ TeV}$ could be a reasonable guestimate of the bilepton mass. A more refined and accurate value of M_Y was nonetheless obtained in [17], where the authors, by using renormalization group arguments, gave the estimate $M_Y = (1.29 \pm 0.06) \text{ TeV}$.

Regarding the new quarks, while in Refs. [4, 5] we assumed that D , S and T were too heavy to contribute to the bilepton width, in this paper we shall instead consider benchmarks wherein non-leptonic decays of bileptons are allowed and explore the yielded final states at LHC and future 100 TeV proton-proton collider. In particular, we shall explore a scenario with all such quarks lighter than $Y^{\pm\pm}$, and another one wherein only D has mass slightly below M_Y , the others being heavier than bileptons.

A study dealing with the phenomenology of TeV-scale quarks T and bileptons was recently carried out in [18]. However, that analysis is somehow complementary to the present one: the authors of [18] explore a scenario with T heavier than doubly- and singly-charged bileptons $Y^{\pm\pm}$ and Y^\pm and, rather than bilepton decays into heavy quarks, as we shall do hereafter, they explore the decays of T into states with $Y^{\pm\pm}$ and Y^\pm , first in a simplified-model framework, recasting the CMS analysis [19], and then in the model of Ref. [1].

Exotic quarks were of course searched at the LHC: in Ref. [19] the CMS collaboration set the limit $M_T > 1.3$ TeV on the mass of heavy quarks T with charge $5/3$, while analyses by ATLAS, such as Ref. [20], led to the bound $M_T > 1.2$ TeV. However, these searches are not directly applicable to our investigation: our TeV-scale quarks carry lepton number $L = 2$ and therefore lead to final states pretty different from those explored in [19, 20] for quarks with $L = 0$. Nevertheless, a study on the primary production of TeV-scale quarks in the bilepton model and the related phenomenology at LHC and future colliders is currently under way [21].

As in Refs. [4, 5], our exploration will account for two reference points, which satisfy the theoretical bounds on the model, as well as the experimental exclusion limits, and investigate the sensitivity of LHC and possibly of the future FCC- hh (pp collisions at $\sqrt{s} = 100$ TeV) to bilepton discovery. In principle, an exhaustive exploration of the reach for bileptons at LHC and ultimately at FCC- hh , varying all model parameters, would be useful and desirable. However, we believe that it would be more appropriate performing this investigation including effects like detector simulations, higher-order corrections to the partonic cross sections and parton distributions, which were not included in Refs. [4, 5] and will not be taken into account in the present paper. We decided to postpone this general analysis to future work [22].

The plan of the present paper is the following. In Section 2 we shall discuss the benchmarks which we choose and the corresponding decay rates and branching ratios of bileptons and new quarks. In Section 3 we will present a phenomenological analysis on bilepton signals and backgrounds at LHC and FCC- hh in our representative points. Finally, Section 4 will contain some concluding remarks on the analysis.

2 Bilepton decays into non-leptonic channels

As discussed in the introduction, this work will deal with the phenomenology of bileptons at LHC and FCC- hh , taking particular care about the decays into the new heavy quarks. For the sake of brevity, we shall omit the theoretical description of the bilepton model, which can be found in the pioneering work [1], as well as in the more recent analyses [4, 5]. We just recall that, as far as new particles beyond the Standard Model are concerned, the model presents four extra neutral scalar Higgs bosons, besides the Standard Model one, for a total of five h_1, \dots, h_5 , three pseudoscalars a_1, a_2 and a_3 , four singly-charged h_1^\pm, \dots, h_4^\pm and three doubly-charged $h_1^{\pm\pm}, h_2^{\pm\pm}$ and $h_3^{\pm\pm}$. The doubly-charged Higgs bosons predicted by the model have lepton number $L = \pm 2$ (scalar bileptons) and the phenomenology of the lightest $H^{\pm\pm}$ was investigated in [5] assuming that it decays into same-sign lepton pairs with 100% branching ratio, namely $1/3$ for each lepton flavour. Furthermore, one has a Z' , which is typically leptophobic, singly- (Y^\pm) and

Benchmark Point BM I (BM II)			
$M_{h_1} = 125.7$	$M_{h_2} = 3213.5$	$M_{h_3} = 5742.4$	$M_{h_4} = 17272.8$
$M_{h_5} = 17348.3$	$M_{a_1} = 5741.0$	$M_{a_2} = 17271.3$	$M_{a_3} = 17348.3$
$M_{h_1^\pm} = 2072.1$	$M_{h_2^\pm} = 5741.7$	$M_{h_3^\pm} = 1727.2$	$M_{h_4^\pm} = 17348.5$
$M_{h_1^{\pm\pm}} = 5397.2$	$M_{h_2^{\pm\pm}} = 17191.7$	$M_{h_3^{\pm\pm}} = 17348.6$	
$M_{Y^{\pm\pm}} = 1288.9$	$M_{Y^\pm} = 1291.0$	$M_{Z'} = 4765.9$	
$M_D = 1000.0$ (1200.0)	$M_S = 1000.0$ (1500.0)	$M_T = 1000.0$ (1500.0)	

Table 1: Particle masses in GeV in benchmark point BM I (BM II).

doubly-charged ($Y^{\pm\pm}$) gauge bileptons, on which the present exploration will be mostly concentrated, as well as quarks with charge $+5/3$ (T) and $-4/3$ (D and S), whose mass will be assumed at the TeV scale.

The goal of this paper is presenting a study of non-leptonic decays of bileptons at LHC and FCC- hh in a couple of representative points of the parameter space, consistent with the theoretical framework and leading to a particle spectrum not yet excluded by the experimental searches. A more general exploration, assessing the dependence of the reach of such accelerators varying all model parameters is currently under way [22].

In order to get an adequate description of the parameter space, we will adopt one benchmark point where all TeV-scale quarks are lighter than the bilepton, and another one with only one quark with mass lower than $M_{Y^{\pm\pm}}$. In both cases, the mass of $Y^{\pm\pm}$ will be fixed about the value estimated in [17]. As in our previous work, the representative points will be obtained after scanning the parameter space by employing the SARAH 4.9.3 [23] code and its UFO interface [24], implementing the latest exclusion limits on physics beyond the Standard Model. Details on the scanning procedure can be found in [5].

A first benchmark, named BM I hereafter, will feature quarks D , S and T with mass about 1 TeV; a second one, labelled BM II, will instead have S and T heavier than $Y^{\pm\pm}$ and D with mass just below M_Y . Limiting ourselves to Higgs and particles beyond the Standard Model, the benchmark mass spectrum is presented in Table 1, where only the masses of D , S and T vary between BM I and BM II and the numbers referring to BM II are quoted in brackets.² From Table 1, one learns that D , S and T have mass 1 TeV in BM I, while in BM II D is slightly lighter than $Y^{\pm\pm}$, i.e. $M_D = 1.2$ TeV,

²Table 1 correctly includes four singly-charged Higgs bosons h_1^\pm, \dots, h_4^\pm , unlike Refs. [4, 5], where the authors omitted in the tables the fourth charged Higgs h_4^\pm .

with the others heavier, i.e. $M_S = M_T = 1.5$ TeV. Moreover, the Standard Model Higgs (h_1) mass is consistent with the LHC observations, while the masses of doubly- and singly-charged bileptons (M_{Y^\pm} and $M_{Y^{\pm\pm}}$) are in agreement with the finding of Ref. [17]. The remaining new particles (Higgs bosons and Z') have mass of a few TeV or higher, and therefore they do not contribute to the bilepton phenomenology which we wish to explore.

Since in this paper we shall study the non-leptonic decays of $Y^{\pm\pm}$ and the subsequent decay chains, it is instructive evaluating widths and branching ratios of bileptons and TeV-scale quarks. For this purpose, we use the `MadGraph` [25] code, which we shall employ in the following for the event simulation too, and in particular its `MadWidth` module [26], at leading order. We obtain:

$$\text{BR}(Y^{++} \rightarrow l^+l^+) \simeq 20.6\% \text{ (BM I)}, 32.5\% \text{ (BM II)}, \quad (1)$$

for each lepton flavour $l = e, \mu, \tau$. As for non-leptonic decays, the branching ratios read:

$$\text{BR}(Y^{++} \rightarrow u\bar{D}, c\bar{S}, T\bar{b}) \simeq 12.7\% \text{ (BM I)}, \text{BR}(Y^{++} \rightarrow u\bar{D}) \simeq 2.5\% \text{ (BM II)}. \quad (2)$$

As expected, in BM I one has substantial branching ratios in all three non-leptonic modes, which clearly lowers the purely leptonic ones. In BM II $Y^{\pm\pm}$ mostly decays into same-sign lepton pairs and it is only the decay with a D quark in the final state which has a small, though non-negligible, rate. Therefore, one can already envisage that it is the BM I scenario the more promising to study non-leptonic decays. Overall, the total bilepton widths read:

$$\Gamma(Y^{\pm\pm}) \simeq 17.9 \text{ GeV (BM I)}; \Gamma(Y^{\pm\pm}) \simeq 11.4 \text{ GeV (BM II)}. \quad (3)$$

The higher bilepton width in BM I is clearly due to the fact that, unlike BM II, decays into channels with S and T quarks are permitted.

In BM I, the TeV-scale quarks exhibit three-body decays into a Standard Model quark and a same-sign lepton pair or a lepton-neutrino pair, through a virtual bilepton. In BM II, S and T are heavier than singly- and doubly-charged bileptons and can therefore decay into final states with a real Y^\pm or $Y^{\pm\pm}$. In BM I the branching ratios of D and S , charged $-4/3$, neglecting light-quark and lepton masses, are independent of quark and lepton flavours and read:

$$\text{BR}(D(S) \rightarrow u(c)l^-l^-) \simeq \text{BR}(D(S) \rightarrow d(s)l^- \nu_l) \simeq 16.7\% \text{ (BM I)}. \quad (4)$$

In BM II, while the D rates are the same as in BM I, i.e. Eq. (4), S can decay into real bileptons as follows:

$$\text{BR}(S \rightarrow cY^{--}) \simeq 50.5\%, \text{BR}(S \rightarrow sY^-) \simeq 49.5\% \text{ (BM II)}. \quad (5)$$

The decay rates of T , which has charge $+5/3$, are instead given by:

$$\text{BR}(T \rightarrow bl^+l^+) \simeq 19.4\%, \quad \text{BR}(T \rightarrow tl^+\bar{\nu}_l) \simeq 13.9\% \quad (\text{BM I}); \quad (6)$$

$$\text{BR}(T \rightarrow bY^{++}) \simeq 64.6\%, \quad \text{BR}(T \rightarrow tY^+) \simeq 35.4\% \quad (\text{BM II}). \quad (7)$$

In BM I the quark T decays into a heavy quark (b or t) plus a lepton pair (two same-sign charged leptons or a charged one and a neutrino) through virtual $Y^{\pm\pm}$ or Y^\pm , with final states with a b quark exhibiting a higher rate. In BM II T decays almost exclusively into a real bilepton and a heavy quark, with the mode bY^{++} being the dominant one. Furthermore, in BM I all TeV-scale quark have a quite small width, of the order of $\mathcal{O}(10^{-3})$ GeV:

$$\Gamma(D) \simeq \Gamma(S) \simeq 3.4 \times 10^{-3} \text{ GeV}, \quad \Gamma(T) \simeq 3.0 \times 10^{-3} \text{ GeV} \quad (\text{BM I}). \quad (8)$$

In BM II, the D width is about $\mathcal{O}(10^{-2})$ GeV, while S and T , being capable of decaying into states with real bileptons, have a larger width of the order of 1 GeV:

$$\Gamma(D) \simeq 1.3 \times 10^{-2} \text{ GeV}, \quad \Gamma(S) \simeq 1.5 \text{ GeV}, \quad \Gamma(T) \simeq 1.1 \text{ GeV} \quad (\text{BM II}). \quad (9)$$

Once the benchmarks have been set and the relevant branching ratios computed, in the next section we shall perform a phenomenological analysis of non-leptonic decays of bileptons at LHC and future colliders, aiming at assessing whether the foreseen cross sections and event numbers are sufficiently high for any signal to be detectable. Whenever this is the case, we shall explore possible observations which allow the discrimination from the Standard Model backgrounds.

Before presenting our result, we point out that, as discussed in our previous paper [5], the bilepton model is perturbative up to a scale about 3.5 TeV [27,28], while the typical scale of $Y^{\pm\pm}Y^{\pm\pm}$ production is $2M_{Y^{\pm\pm}}$, i.e. about 2.6 TeV in our case. Therefore, we shall assume that a perturbative analysis is legitimate in the energy regime of the present work.

3 Phenomenological analysis

In this section we shall investigate the phenomenology of bilepton non-leptonic decays in our two benchmark points at the LHC, i.e. pp collisions at a centre-of-mass energy $\sqrt{s} = 13$ TeV and integrated luminosity $\mathcal{L} = 300 \text{ fb}^{-1}$, and at a future hadron colliders (FCC- hh) with $\sqrt{s} = 100$ TeV and $\mathcal{L} = 3000 \text{ fb}^{-1}$. An extension of the 13 TeV results to the high-luminosity LHC (HL-LHC), namely $\sqrt{s} = 14$ TeV and $\mathcal{L} = 3000 \text{ fb}^{-1}$ is straightforward too.

As discussed in the previous section, hereafter we shall use the `MadGraph` code in the leading-order approximation, deferring the inclusion of NLO corrections to future work. Through our work, we shall employ the NN23LO1 set of LO parton distribution functions [29], while parton showers and hadronization will be simulated by the `HERWIG 6` code [30].

For bileptons at 1.29 TeV, the cross sections for pair production are given by:

$$\sigma(pp \rightarrow Y^{++}Y^{--}) \simeq 0.75 \text{ fb (LHC, 13 TeV);} \quad (10)$$

$$\sigma(pp \rightarrow Y^{++}Y^{--}) \simeq 1.12 \text{ fb (LHC, 14 TeV);} \quad (11)$$

$$\sigma(pp \rightarrow Y^{++}Y^{--}) \simeq 393.89 \text{ fb (FCC-}hh\text{).} \quad (12)$$

As easily predictable, the FCC- hh cross section is about 500 and 350 times larger than the LHC one at 13 and 14 TeV, respectively.

In the scenario BM I, as a case study, we will investigate $Y^{\pm\pm}$ primary decays into quarks T , which then decay into a bottom quark and a same sign lepton pair. Limiting for simplicity our exploration to one lepton species, such as muons, which have a better charge identification than electrons at LHC (see, e.g., Refs. [31,32]), this corresponds to the following process³:

$$pp \rightarrow Y^{++}Y^{--} \rightarrow (T\bar{b})(\bar{T}b) \rightarrow (b\bar{b}\mu^+\mu^+)(b\bar{b}\mu^-\mu^-) \text{ (BM I),} \quad (13)$$

which lead to final states with four b -flavoured jets and four muons ($4b4\mu$). In Fig. 1 (left) we display an example of the decay chain (13), assuming a primary $Y^{++}Y^{--}$ production via quark-antiquark annihilation, with the exchange of a neutral boson V^0 (photon, Z , Z' or any electrically-neutral Higgs). For the sake of comparison, in Fig. 1 (right) we also present a companion diagram, accounted for in [4,5], where bileptons decay into same-sign muon pairs.⁴

In reference point BM II, we shall instead analyze primary decays involving TeV-scale quarks D and yielding final states with four u -quark initiated light jets accompanied by four muons ($4u4\mu$):

$$pp \rightarrow Y^{++}Y^{--} \rightarrow (\bar{D}u)(D\bar{u}) \rightarrow (u\bar{u}\mu^+\mu^+)(u\bar{u}\mu^-\mu^-) \text{ (BM II).} \quad (14)$$

A representative diagram of process (14) can be obtained from Fig. 1 (left), after replacing T with D and b with u .

³Of course, if we account for both electrons and muons, we will have to roughly double cross sections and event rates at LHC and FCC- hh .

⁴We point out that Fig. 1 shows only a particular contribution to bilepton production and decay in a pp collision. The `MadGraph` code calculates all diagrams allowed by the bilepton model, including, for example, the production of $Y^{++}Y^{--}$ mediated by the exchange of a TeV-scale quark in the t -channel.

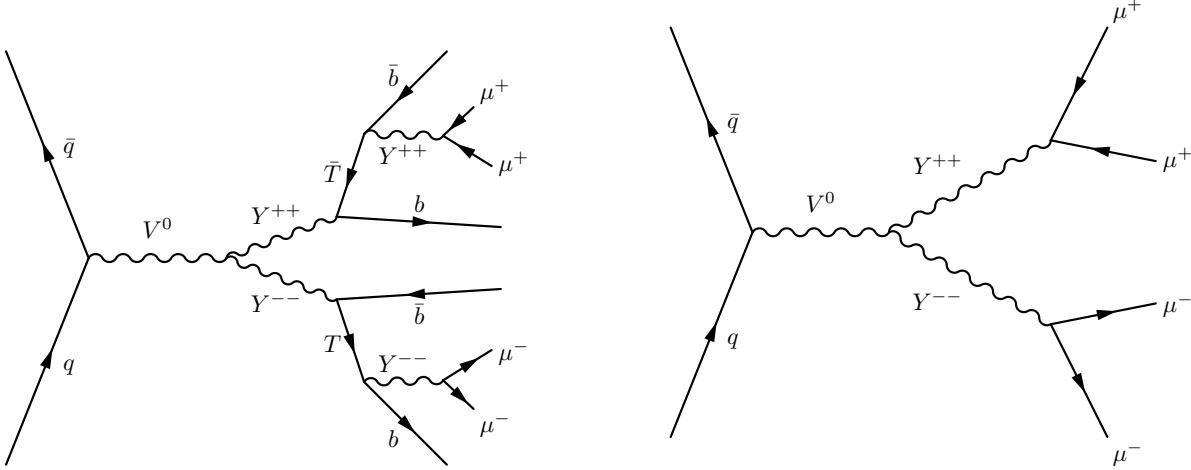


Figure 1: Left: example of diagram leading to the decay chain (13), investigated in the present paper. Right: Pair-production of bileptons decaying into same-sign muons, explored in [4, 5].

An upper limit on the predicted number of events at LHC and FCC- hh can be estimated by multiplying the inclusive cross sections in Eqs. (10)–(12) by the relevant branching ratios, assuming a perfect tagging efficiency and no cut on final-state jets and leptons. Implementing the branching ratios of bileptons and TeV-scale quarks in Eqs. (1)–(7), we obtain that the leading-order (LO) cross sections of the chain (13) at 13 and 14 TeV centre-of-mass energies read:

$$\sigma(pp \rightarrow YY \rightarrow 4b4\mu) \simeq 4.55 \times 10^{-4} \text{ fb (LHC, 13 TeV, BM I);} \quad (15)$$

$$\sigma(pp \rightarrow YY \rightarrow 4b4\mu) \simeq 6.80 \times 10^{-4} \text{ fb (LHC, 14 TeV, BM I).} \quad (16)$$

Such cross sections are clearly too small to see any event at 300 fb^{-1} and even at 3000 fb^{-1} (HL-LHC). At FCC- hh one instead has:

$$\sigma(pp \rightarrow YY \rightarrow 4b4\mu) \simeq 0.24 \text{ fb (FCC-}hh\text{, BM I),} \quad (17)$$

hence a few hundred events can be foreseen at 3000 fb^{-1} . Regarding the BM II scenario, namely the decay chain (14), the prediction for the LHC leads to cross sections of $\mathcal{O}(10^{-5} \text{ fb})$ hence too low for any analysis to be worthwhile at either 300 or 3000 fb^{-1} :

$$\sigma(pp \rightarrow YY \rightarrow 4u4\mu) \simeq 1.31 \times 10^{-5} \text{ fb (LHC, 13 TeV, BM II),} \quad (18)$$

$$\sigma(pp \rightarrow YY \rightarrow 4u4\mu) \simeq 2.03 \times 10^{-5} \text{ fb (LHC, 14 TeV, BM II),} \quad (19)$$

If one refers instead to FCC- hh , the cross section for the production of four light jets and four muons through the process in Eq. (14) is given by:

$$\sigma(pp \rightarrow YY \rightarrow 4u4\mu) \simeq 6.87 \times 10^{-3} \text{ fb (FCC-}hh\text{, BM II).} \quad (20)$$

It is therefore a less promising scenario than BM I even at FCC- hh , but it is still worthwhile checking whether any signal, though small, could be separated from the background.

Before presenting any phenomenological distribution, we need to account for the backgrounds mimicking the bilepton signal, and set acceptance cuts on both signal and backgrounds. Because of the expected statistics, we shall limit ourselves to the FCC- hh case. As for the chain (13), leading to four b -jets and four muons, we shall consider the primary production of four b quarks and two Z bosons decaying into muon pairs (background b_1):

$$pp \rightarrow b\bar{b}b\bar{b}ZZ \rightarrow b\bar{b}b\bar{b}\mu^+\mu^-\mu^+\mu^-. \quad (21)$$

We shall also investigate the production of four top quarks, with the subsequent W 's decaying into muons and requiring, as in [4], a small missing energy due to the muon neutrinos (background b_2):

$$pp \rightarrow t\bar{t}t\bar{t} \rightarrow (bW^+)(bW^+)(\bar{b}W^-)(\bar{b}W^-) \rightarrow b\bar{b}b\bar{b}\mu^+\mu^-\mu^-\mu^-\nu_\mu\nu_\mu\bar{\nu}_\mu\bar{\nu}_\mu. \quad (22)$$

The above background deserves some further comments. Four-top production occurs mostly through QCD-mediated processes; however, it was recently found [33] that electroweak contributions, at both LO and NLO, are non-negligible as they can have an impact up to 10% on the total cross section and even larger on differential distributions. Therefore, we modified the default four-top `MadGraph` LO generation, which includes only QCD interactions, and accounted for the electroweak contributions as well. Furthermore, as discussed in [34, 35], the analyses on four-top searches at LHC can be recast to set bounds on several new physics models. In particular, Ref. [34] recasts the CMS search [36] at 35.9 fb^{-1} to constrain the sgluon mass, while Ref. [35] reinterprets the analysis [37] in terms of top-philic simplified-model scalar/vector singlets or octets (see also [38] for the actual implementation in the `MadAnalysis` framework [39]). Such studies tend therefore to suggest that one may even recast the analyses [36, 37] in terms of the bilepton model at LHC and FCC- hh : this is nevertheless deferred to future work.

Although they are supposed to give a less significant contribution to the background than processes (21) and (22), we shall also account for four light jets and two Z bosons decaying into muon pairs (background b_3), i.e.

$$pp \rightarrow jjjjZZ \rightarrow jjjj\mu^+\mu^-\mu^+\mu^-. \quad (23)$$

as well as processes with two light jets, two b -jets and two $Z \rightarrow \mu^+\mu^-$ (b_4), namely

$$pp \rightarrow jjb\bar{b}ZZ \rightarrow jjb\bar{b}\mu^+\mu^-\mu^+\mu^-, \quad (24)$$

where we assume that j is either a light-quark or gluon-initiated jet, mistagged as a b -jet.

Concerning the other scenario, i.e. the decay chain (14) in BM II, the main background is the process in Eq. (23), i.e. four light jets and two Z bosons decaying into muons (b_3).

In our phenomenological analysis, along the lines of [4, 5], we cluster jets according to the k_T algorithm [40] with a radius-like parameter $R = 1$ and apply the following acceptance cuts on jets and muons:

$$\begin{aligned}
p_{T,j} > 30 \text{ GeV}, \quad p_{T,\mu} > 20 \text{ GeV}, \quad |\eta_j| < 4.5, |\eta_\mu| < 2.5, \\
\Delta R_{jj} > 0.4, \quad \Delta R_{\mu\mu} > 0.1, \quad \Delta R_{j\mu} > 0.4, \quad \text{MET} < 200 \text{ GeV}.
\end{aligned}
\tag{25}$$

As pointed out in [5], the cuts in Eq. (25) correspond to a conservative choice of the overlap-removal algorithm implemented to discriminate lepton and jet tracks at LHC [41, 42]. The cut $\text{MET} < 200 \text{ GeV}$ refers to the missing transverse energy, i.e. $\text{MET} = \sqrt{(\sum_{i=\nu} p_{x,i})^2 + (\sum_{i=\nu} p_{y,i})^2}$, due to the neutrinos in the final state.⁵

In principle, for the sake of a reliable analysis, one should implement the b -tagging efficiency, as well as the probability of mistagging a jet as a b -jet. Also, in principle such efficiencies depend in the jet rapidity and transverse momentum, as well as on the flavour of the parton which originates the jet. However, in this explorative letter, in first approximation we shall implement such effects in a flat manner, i.e. independently of the jet kinematics, and defer to future work any rigorous and systematic inclusion of the tagging rates. Following Ref. [43], we shall assume the following b -tagging efficiency (ϵ_b) and mistag rate (ϵ_j)⁶:

$$\epsilon_b = 0.82, \quad \epsilon_j = 0.05.
\tag{26}$$

Before presenting our results, it is mandatory to calculate the cross section and the number of events foreseen at FCC- hh , after the cuts (25) and the efficiencies (26) are imposed, for both signal and backgrounds. Overall, one can envisage that, unlike Refs. [4, 5], where the signal final states were purely leptonic and all leptons, coming from the decay of a heavy resonance, had a sufficiently large transverse momentum to pass the cuts, our signal and background processes, involving both jets and leptons coming from more complex decay chains, should feel a stronger effect and a more severe suppression due to the cuts. From a more technical viewpoint, we set some basic looser cuts at the level of the matrix-element generation with `MadGraph` and the stronger cuts in

⁵The $\text{MET} < 200 \text{ GeV}$ cut should be applied to the neutrinos in W decays in the 4-top background (22) and, for the sake of consistency, to all neutrinos produced in hadron decays in both signal and backgrounds. Nevertheless, we checked that neutrinos from hadron decays are much softer than those in top decays, so that they are almost unaffected by the MET cut.

⁶Strictly speaking, our efficiencies refer to jets with pseudorapidity $|\eta_j| < 2.5$ and transverse momentum $10 \text{ GeV} < p_{T,j} < 500 \text{ GeV}$, which roughly correspond to the region where most events occur. Furthermore, according to [43], the mistag rate runs from 0.01 (jets initiated by u, d, s quarks or gluons) to 0.15 (charm-flavoured jets). Our value $\epsilon_j = 0.05$ represents therefore a sort of weighted average between these two extreme values.

(25) after the matching with HERWIG. In fact, without setting any cut at parton level, processes like the backgrounds (21)–(22) would be divergent because of the soft and collinear singularities. For a review on matching matrix elements and parton showers for multi-jet events see Ref. [44].

As for process (13), we find that, after the acceptance cuts are accounted for, the signal (s) cross section amounts to $\sigma(4b4\mu)_s \simeq 6.24 \times 10^{-2}$ fb. Including the b -tagging efficiency as in Eq. (26), one can then envisage $N(4b4\mu)_s \simeq 90$ events at FCC- hh for a luminosity $\mathcal{L} = 3000 \text{ fb}^{-1}$. As for the backgrounds (21)–(24), after all cuts, as well as b -tagging and mistag rates are applied, we obtain $\sigma(4b4\mu)_{b_1} \simeq 1.28 \times 10^{-2}$ fb, $\sigma(4b4\mu + \text{MET})_{b_2} \simeq 3.34 \times 10^{-2}$ fb, $\sigma(4j4\mu)_{b_3} \simeq 4.43$ fb, $\sigma(2b2j4\mu)_{b_4} \simeq 1.34$ fb. Multiplying such cross sections by the luminosity, accounting for the tagging efficiencies and rounding to the nearest ten, the expected number of events are then given by $N(4b4\mu)_{b_1} \simeq 20$, $N(4b4\mu + \text{MET})_{b_2} \simeq 50$, while backgrounds b_3 and b_4 yield too few events to be significant at FCC- hh .

Regarding BM II and the decay chain (14), the cross section after the cuts is about $\sigma(4j4\mu)_s \simeq 1.88 \times 10^{-3}$ fb, FCC- hh . As a result, considering that some extra suppression is to be expected at FCC- hh due, e.g., to the efficiency of jet/lepton tagging, which will further lower the event rate of process (14), we prefer to neglect the BM II scenario and concentrate ourselves on BM I, namely the decay chain (13) and its main backgrounds (21) and (22).

In our phenomenological analysis, we shall investigate the following observables: the transverse momentum of the hardest ($p_{T,1}$) and next-to-hardest ($p_{T,2}$) muons, the hardest-muon pseudorapidity η_1 , the invariant mass $M_{\mu\mu}$ of same-sign muons, the polar angle between same-sign muons $\theta_{\mu\mu}$, the invariant opening angle $\Delta R_{\mu\mu} = \sqrt{(\Delta\phi)^2 + (\Delta\eta)^2}$ between hardest and next-to-hardest muons, ϕ being the muon azimuth, the transverse momentum of the two hardest jets, $p_{T,j1}$ and $p_{T,j2}$, also named as first and second jet, which in our final states are b -flavoured, the invariant opening angle between first jet and hardest muon ($\Delta R_{j\mu}$) and between the two hardest jets (ΔR_{jj}).

In Figs. 2–6 we present the distributions resulting from our investigation: everywhere, our histograms are normalized in such a way that the height of each bin, say $N(x)$, represents the foreseen number of events at x at FCC- hh . Figure 2 displays the spectra of the transverse momenta of the hardest ($p_{T,1}$, left) and next-to-hardest muon ($p_{T,2}$, right) according to the signal (13) and backgrounds (21) and (22). The muon p_T spectra look quite similar: the backgrounds are substantial only at low transverse momentum, peak about $p_{T,1} \simeq 100$ GeV and $p_{T,2} \simeq 60$ GeV and rapidly vanish at large p_T , in such a way that for $p_{T,1} > 500$ GeV and $p_{T,2} > 300$ GeV only the signal survives. On the contrary, the signal distributions are pretty broad and yield some events up to $p_{T,1} \simeq 2$ TeV and $p_{T,2} \simeq 1.5$ TeV. Requiring therefore muons with transverse momenta above a few hundred GeV would therefore help to discriminate the signal from the

background: this was of course quite predictable, since, unlike the backgrounds, our signal muons are indirectly related to the decay of a TeV-scale resonance, and therefore a large p_T is to be expected.

Regarding Fig. 3, where the invariant mass of same-sign muons $M_{\mu\mu}$ (left) and the invariant opening angle $\Delta R_{\mu\mu}$ (right) between the two hardest muons are presented, one can learn that, unlike the backgrounds, whose $M_{\mu\mu}$ prediction peaks at low values and becomes negligible above 500 GeV, the signal yields a quite broad $M_{\mu\mu}$ spectrum, which is shifted towards large values and peaks at around 700 GeV. As for $\Delta R_{\mu\mu}$, the signal is well above the backgrounds in the whole range $0 < \Delta R_{\mu\mu} < 6$ and peaks at $\Delta R \simeq 3$. The background b_1 exhibits a rather flat $\Delta R_{\mu\mu}$ distribution, while b_2 has a $\Delta R_{\mu\mu}$ spectrum with a shape similar to the signal, though yielding a lower number of events in every bin.

Figure 4 displays the angle $\theta_{\mu\mu}$ (left) between the two hardest muons and the pseudorapidity η_1 (right) of the hardest one. For the purpose of $\theta_{\mu\mu}$, the signal spectrum is broad, peaks at $\theta_{\mu\mu} \simeq 0.8$ and is well above the backgrounds up to $\theta_{\mu\mu} \simeq 1.8$. The backgrounds have a spectrum which is rather flat, while for large angles, say $\theta_{\mu\mu} > 2$, the four-top background b_2 yields the highest rate of events, above both signal and background b_1 . Concerning the pseudorapidity distribution, regardless of the normalization, the shape of signal and background b_1 are similar, with b_1 just predicting events with $|\eta| < 1.8$. The background b_2 exhibits instead a quite flat η distribution for $|\eta| < 1.5$ and is even above the signal for $1.5 < |\eta| < 2.5$.

In Figs. 5 and 6 we instead explore the b -jet properties, and in particular the transverse momenta $p_{T,j1}$ and $p_{T,j2}$ of the first and second b -jet (Fig. 5) and the invariant opening angles ΔR_{jj} and $\Delta R_{\mu j}$ between the two hardest jets and between hardest jet and hardest muon (Fig. 6). Overall, the comparison is similar to what was observed for the leptonic observables. While background jets typically peak at small transverse momenta, about $p_T \simeq 60$ GeV (b_1) and $p_T \simeq 1000$ GeV (b_2) and vanish for $p_T > 400$ GeV, the spectra yielded by the b -jets originated from non-leptonic bilepton decays are rather broad, dominate over the backgrounds above 300 GeV and give meaningful event rates up to about 1.2 TeV.

Concerning the invariant opening angles plotted in Fig. 6, unlike the transverse momentum distributions, the shapes are more similar and the difference among the spectra is mostly due to the overall normalization, with the signal dominating over b_1 and b_2 for $\Delta R_{j\ell} < 4.5$ and $\Delta R_{jj} < 3.5$. For larger opening angles the backgrounds tend to become competitive with the signal and it is in fact b_2 which yields the highest rate for $\Delta R_{j\ell} > 4.5$ and $\Delta R_{jj} > 3.5$.

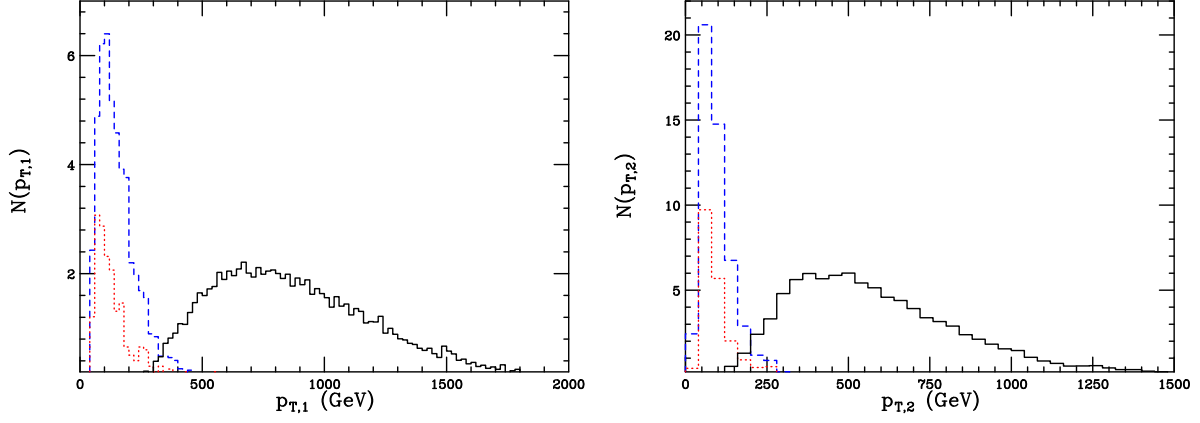


Figure 2: Transverse momentum of the hardest (left) and next-to-hardest muon (right) for the bilepton signal (solid) and the backgrounds with four top quarks (dashes) and two b quarks and two Z bosons decaying to muons (dots).

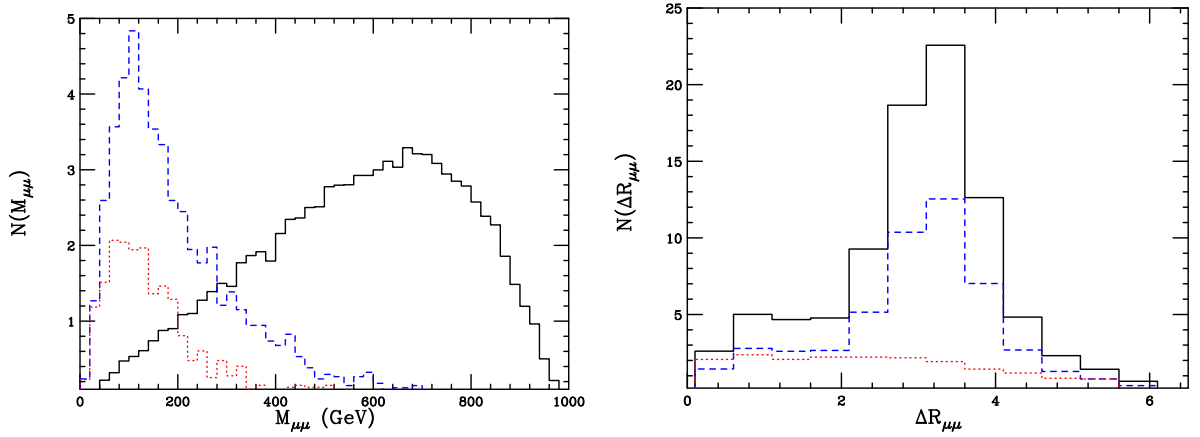


Figure 3: Left: invariant mass of same-sign muons. Right: Invariant opening angle ΔR between the two hardest muons. The histograms refer to signal and backgrounds according to the convention in Fig. 2

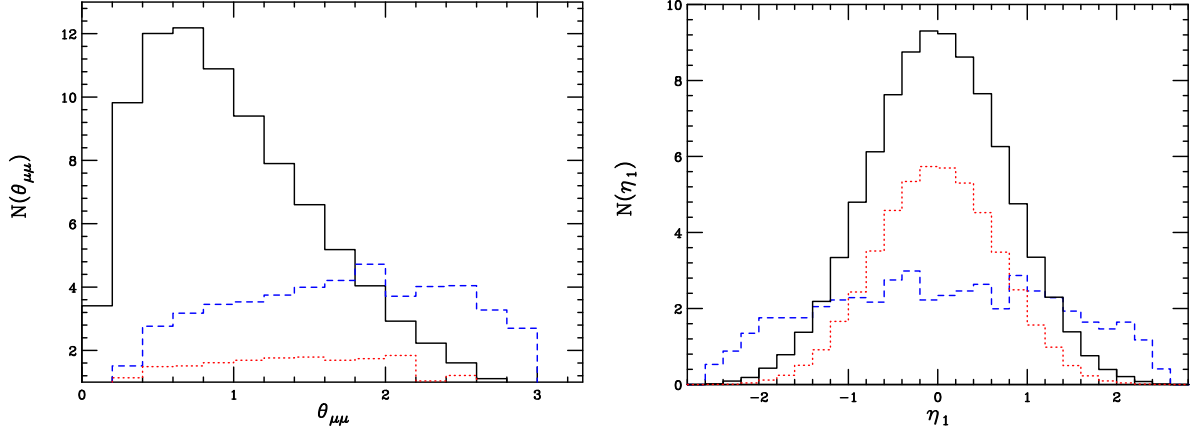


Figure 4: Angle between the two hardest muons (left) and rapidity of the hardest muons. Histogram styles as in the previous figures.

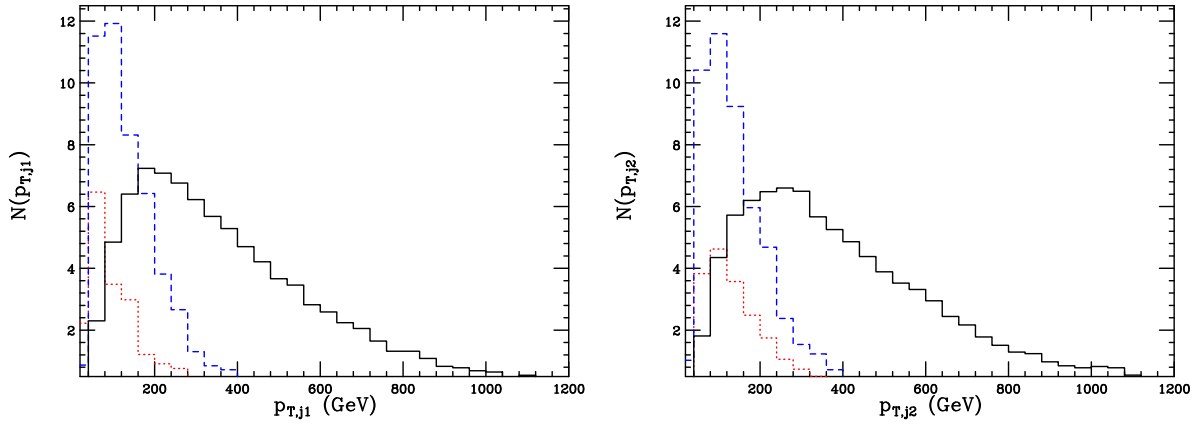


Figure 5: First- (left) and second-jet (right) transverse momentum, for the bilepton signal (solid) and Standard Model backgrounds (dots and dashes).

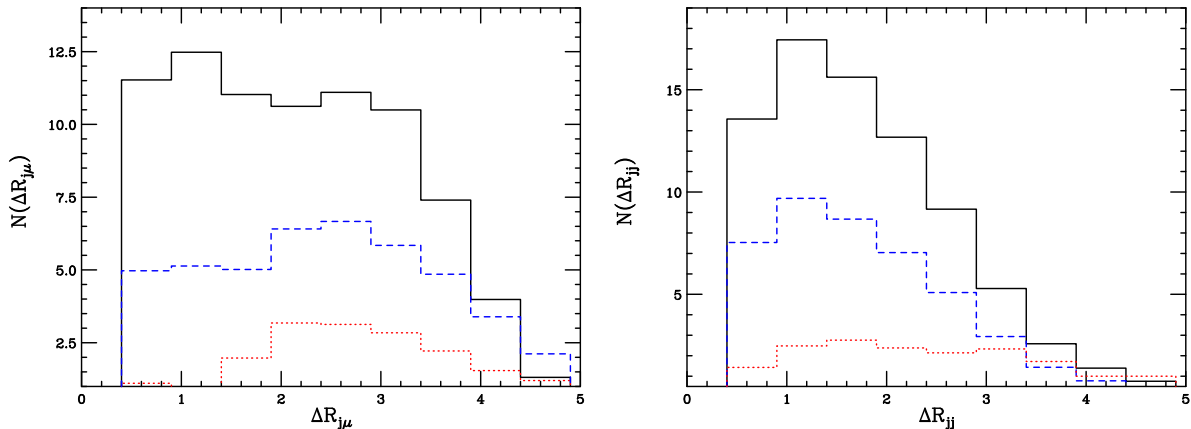


Figure 6: As in Figs. 2–5, but displaying the invariant opening angle between the hardest jet and the hardest muon (left) and the between first and second jet (right).

4 Conclusions

We investigated the phenomenology of gauge bileptons $Y^{\pm\pm}$, as predicted in the model [1], based on a 331 group structure, paying special attention to their non-leptonic decays in channels containing new TeV-scale quarks. We chose two benchmark points consistent with the current exclusion limits on the searches for physics beyond the Standard Model and with the bilepton mass estimate given in [17], and explored bilepton phenomenology at LHC and at a future 100 TeV collider FCC- hh .

We found that the cross sections are too low for any signal of non-leptonic decays of bileptons to be visible at LHC, at either 13 TeV and a luminosity of 300 fb^{-1} or 14 TeV and $\mathcal{L} = 3000 \text{ fb}^{-1}$. Our first conclusion is therefore that, for the time being, the LHC can detect bileptons only searching for same-sign lepton pairs, along the lines of Refs. [4, 5], while the statistics are not sufficient to be sensitive to decays into new TeV-scale heavy quarks. Nevertheless, non-leptonic bilepton decays could be observed at the FCC- hh in a scenario wherein all three new quarks are slightly lighter than the bilepton itself. For this purpose, we explored decay chains leading to four b -flavoured jets and four muons through the primary production of bilepton pairs $Y^{++}Y^{--}$ decaying into quarks with charge $\pm 5/3$. The backgrounds due to two $t\bar{t}$ pairs, with all top quarks decaying leptonically, or two $b\bar{b}$ pairs and two Z bosons, eventually leading to two muon pairs were investigated as well. We found that the signal can be discriminated at FCC- hh , since it typically leads to events with muons and jets at large p_T and same-sign muon pairs with high invariant mass which dominate over the background in most phase space.

In summary, in the present study we have demonstrated that it can be worth considering non-leptonic decays of bileptons, but one would need to wait for the very high-

energy FCC- hh for any realistic search. Ideally, if the LHC were to have any bilepton signal in the same-sign lepton-pair channel, then a 100 TeV collider could shed further light on the model, as it could reveal even the TeV-scale quarks (see also Ref. [45]), which represent another striking feature of the bilepton scenario.

Of course, this paper and our previous work in [4, 5] can still be extended according to several guidelines. In fact, we plan to include in our investigation effects like detector simulations, realistic tagging efficiencies for jets and leptons at LHC and FCC- hh , as well as higher-order corrections to the partonic cross section and parton distribution functions. After accounting for such effects one could then give a realistic estimate of the sensitivity of LHC and FCC- hh to bileptons in the various decay channels as a function of the most relevant model parameters. Furthermore, as pointed out when discussing the backgrounds, the four-top searches can be recast in terms of the bilepton model from the LHC to the FCC- hh energies. Finally, it is obviously very interesting exploring the primary production of TeV-scale quark pairs in the bilepton model and their subsequent decays into bileptons, assuming that the heavy quarks are heavier than $Y^{\pm\pm}$. This is in progress as well.

Acknowledgements

We acknowledge Marco Zaro and Jack Araz for discussions on the MadGraph simulation. We also thank Marianna Testa, Antonio Sidoti and Giacomo Polesello for advices concerning the acceptance cuts on jets and leptons and the b -tagging efficiency.

References

- [1] P.H. Frampton,
Chiral Dilepton Model and the Flavor Question,
Phys. Rev. Lett. **69**, 2889 (1992).
- [2] F. Pisano and V. Pleitez,
An $SU(3) \times U(1)$ Model for Electrode Interactions,
Phys. Rev. **D46**, 410 (1992).
- [3] P.H. Frampton,
Narrow Resonance in e^-e^- Scattering due to Additional Gauge Boson,
Int. J. Mod. Phys. **A11**, 1621 (1996).
- [4] G. Corcella, C. Corianò, A. Costantini and P.H. Frampton,
Bilepton Signatures at the LHC,

- Phys. Lett. **B773**, 544 (2017),
arXiv:1707.01381 [hep-ph].
- [5] G. Corcella, C. Corianò, A. Costantini and P.H. Frampton,
Exploring Scalar and Vector Bileptons at the LHC in a 331 Model,
Phys. Lett. **B785**, 73 (2018),
arXiv:1806.04536 [hep-ph].
- [6] A. Alloul, M. Frank, B. Fuks and M. Rausch de Traubenberg,
Doubly-charged particles at the Large Hadron Collider,
Phys. Rev. **D88** (2013) 075004.
arXiv:1307.1711 [hep-ph]
- [7] L. Willmann, *et al.*,
New Bounds from Searching for Muonium to Antimuonium Conversion,
Phys. Rev. Lett. **83**, 49 (1999),
arXiv:hep-ex/9807011.
- [8] E.D. Carlson and P.H. Frampton,
Lower Bound on Dilepton Mass from Polarized Muon Decay,
Phys. Lett. **B283**, 123 (1992),
- [9] J.R. Musser, *et al.*,
Measurement of the Michel Parameter in Muon Decay.
Phys. Rev. Lett. **94**, 101805 (2005),
arXiv:hep-ex/0409063.
- [10] R. Prieels, *et al.*,
Measurement of the Michel Parameter in Polarized Muon Decay,
Phys. Rev. **D90**, 112003 (2014).
arXiv:1408.1472 [hep-ex].
- [11] ATLAS Collaboration,
Search for Doubly Charged Higgs Boson Production in Multi-Lepton Final States with the ATLAS Detector Using Proton-Proton Collisions at $\sqrt{s} = 13$ TeV,
Eur. Phys. J. **C78** (2018) 199.
- [12] CMS Collaboration,
A Search for Doubly-Charged Higgs Boson Production in Three and Four Lepton Final States at $\sqrt{s} = 13$ TeV,
CMS-PAS-HIG-16-036.
- [13] J. C. Pati and A. Salam,
Lepton Number as the Fourth Color ,
Phys. Rev. **D10** (1974) 275, Erratum: Phys. Rev. **D11** (1975) 70.

- [14] R. N. Mohapatra and J. C. Pati,
Left-Right Gauge Symmetry and an Isoconjugate Model of CP Violation,
Phys. Rev. **D11** (1975) 566.
- [15] M. Muhlleitner and M. Spira,
Note on Doubly Charged Higgs Pair Production at Hadron Colliders,
Phys. Rev. **D68** (2003) 117701.
arXiv:hep-ph/0305288
- [16] ATLAS Collaboration,
Search for Doubly and Singly Charged Higgs Bosons Decaying into Vector Bosons in Multi-lepton Final States with the ATLAS Detector Using Proton-Proton Collisions at $\sqrt{s} = 13$ TeV,
JHEP **2106** (2021) 146.
arXiv:2101.11961 [hep-ex].
- [17] C. Corianò and P.H. Frampton,
Refined Mass Estimate for Bilepton Gauge Boson,
Mod. Phys. Lett. **A36** 2050118.
arXiv:2011.02037 [hep-ph].
- [18] A. Costantini, G. Corcella, M. Ghezzi, G.M. Pruna, L. Panizzi and J. Salko,
Vector-like quarks decaying into singly and doubly charged bosons at LHC,
JHEP **2110** (2021) 108.
arXiv:2107.07426 [hep-ph].
- [19] CMS Collaboration,
Search for top quark partners with charge 5/3 in the same-sign dilepton and single-lepton final states in proton-proton collisions at $\sqrt{s} = 13$ TeV,
JHEP **1903** (2019) 082.
arXiv:1810.03188 [hep-ex].
- [20] ATLAS Collaboration, *Search for new phenomena in events with same-charge leptons and b-jets in pp collisions at $\sqrt{s} = 13$ TeV with the ATLAS detector*.
JHEP **1812** (2018) 039.
arXiv:1807.11883 [hep-ex].
- [21] G. Corcella, C. Corianò, A. Costantini, P.H. Frampton,
TeV-scale heavy quark production in the bilepton model,
work in progress.
- [22] J.Y. Araz, G. Corcella, C. Corianò, A. Costantini, P.H. Frampton,
A phenomenological analysis of bilepton production and decay at LHC and FCC,
work in progress.

- [23] F. Staub,
SARAH 4 : A Tool for (not only SUSY) Model Builders,
Comput. Phys. Commun. **185** (2014) 1773.
arXiv:1309.7223 [hep-ph]
- [24] C. Degrande *et al.*,
UFO - The Universal FeynRules Output,
Comput. Phys. Commun. **183** (2012) 1201.
arXiv:1108.2040 [hep-ph]
- [25] J. Alwall *et al.*,
The Automated Computation of Tree-Level and Next-to-leading Order Differential Cross Sections, and their Matching to Parton Shower Simulations,
JHEP **1407** (2014) 079.
1405.0301 [hep-ph]
- [26] J. Alwall *et al.*,
Computing decay rates for new physics theories with FeynRules and MadGraph5_aMC@NLO,
Comput. Phys. Commun. **197** (2015) 312.
arXiv:1402.1178 [hep-ph]
- [27] A.G. Dias, R. Martinez and V. Pleitez,
Concerning the Landau pole in 3-3-1 models,
Eur. Phys. **C39** (2005) 101.
arXiv:hep-ph/0407141
- [28] R. Martinez and F. Ochoa,
The Landau pole and Z' decays in the 331 dilepton model,
Eur. Phys. **C51** (2005) 701.
arXiv:hep-ph/0606173
- [29] NNPDF Collaboration,
Theoretical issues in PDF determination and associated uncertainties,
Nucl. Phys. **B874** (2013) 36.
- [30] G. Corcella *et al.*,
HERWIG 6: An Event Generator for Hadron Emission Reactions with Interfering Gluons (Including Supersymmetric Processes),
JHEP **0101** (2001) 010.
arXiv:hep-ph/0011363
- [31] ATLAS Collaboration,
Muon Reconstruction and Identification Efficiency in ATLAS Using the Full Run

2 pp Collision Data Set at $\sqrt{s} = 13$ TeV,
ATLAS-CONF-2020-030.

- [32] ATLAS Collaboration,
Electron Reconstruction and Identification in the ATLAS Experiment Using the 2015 and 2016 LHC Proton-Proton Collision Data at $\sqrt{s} = 13$ TeV,
Eur. Phys. J. **C79** (2019) 639.
- [33] R. Frederix, D. Pagani and M. Zaro,
Large NLO corrections in $t\bar{t}W^\pm$ and $t\bar{t}t\bar{t}$ hadroproduction from supposedly subleading EW contributions,
JHEP **1802** (2018) 031.
arXiv:1711.02116 [hep-ph]
- [34] L. Darmé, B. Fuks and M. Goodsell,
Cornering sgluons with four-top-quark events,
Phys. Lett. **B784** (2018) 223.
arXiv:1805.10835 [hep-ph]
- [35] L. Darmé, B. Fuks and F. Maltoni,
Top-philic heavy resonances in four-top final states and their EFT interpretation,
JHEP **2021** (2020) 143.
arXiv:2104.09512 [hep-ph]
- [36] CMS Collaboration,
Search for standard model production of four top quarks with same-sign and multi-lepton final states in proton-proton collisions at $\sqrt{s} = 13$ TeV,
Eur. Phys. J. **C78** (2018) 140.
- [37] CMS Collaboration,
Search for production of four top quarks with same-sign and multiple lepton final states in proton-proton collisions at $\sqrt{s} = 13$ TeV,
Eur. Phys. J. **C80** (2020) 75.
- [38] L. Darmé and B. Fuks,
Implementation of the CMS-TOP-18-003 analysis in the MadAnalysis 5 framework (four top quarks with at least two leptons; 137 fb^{-1}),
Mod. Phys. Lett. **A36** (2021) 01 2141008.
- [39] E. Conte, B. Fuks and G. Serret,
MadAnalysis 5, A User-Friendly Framework for Collider Phenomenology,
Comput. Phys. Commun. **184** (2013) 222.
arXiv:1206.1599 [hep-ph]

- [40] S. Catani, Yu.L. Dokshitzer, M.H. Seymour and B.R. Webber,
Longitudinally Invariant k_t Clustering Algorithms for Hadron-Hadron Collisions,
Nucl. Phys. **B406** (1993) 187.
- [41] ATLAS Collaboration,
*Search for squarks and gluinos in events with hadronically decaying tau leptons, jets
and missing transverse momentum in proton–proton collisions at $\sqrt{s} = 13$ GeV
recorded with the ATLAS detector*,
Eur. Phys. J. **C76** (2016) 683.
- [42] G. Polesello, private communication.
- [43] M. Selvaggi,
A Delphes parametrisation of the FCC-hh detector,
CERN-FCC-PHYS-2020-0003.
- [44] J. Alwall et al,
*Comparative study of various algorithms for the merging of parton showers and
matrix elements in hadronic collisions*,
Eur. Phys. J. **C53** (2008) 473.
arXiv:0706.2569 [hep-ph]
- [45] P.H. Frampton,
Additional Baryons and Mesons,
Mod. Phys. Lett. **A36** 2150179 (2021).
arXiv:2108.10730 [hep-ph]